ANALYTICAL METHOD DEVELOPMENT AND FUNDAMENTAL STUDIES ON THE SEPARATION OF DRUGS USING CAPILLARY ELECTROPHORESIS

by

KHALDUN MOHAMMAD MITLAQ AL AZZAM

Thesis submitted in fulfillment of the requirements for the degree of Doctor of Philosophy

2011

Acknowledgements

First and foremost, I would like to express my unlimited sincere gratitude to my supervisor, Professor Bahruddin Saad for his supervision, guidance and patience throughout the course of my study during these few years. His understanding, expertise and patience, expertise in guiding students, helped me massively in overcoming the difficulties encountered during the course of my study and in completing the thesis. His infinite knowledge, enthusiasm and attention to detail have added considerably to my graduate experience and continue to inspire my curiosity and creativity in scientific research. He has always given me the freedom to plan and execute the research plans, and to develop myself. His wonderful personality has and will continue to influence and shape my behavior throughout my life.

Also, it is a great pleasure to thank Professor Hassan Y. Aboul-Enein (Pharmaceutical and Medicinal Chemistry Department, National Research Centre, Cairo, Egypt) for discussions on chiral work and for providing some drugs for analysis, Dr. Abdalla Ahmed Elbashir, (Khartoum University, Faculty of Science, Chemistry Department), for his valued advises and discussions, Associate Professor Dr. Rohana Adnan and her student Norariza Ahmad, (School of Chemical Sciences, USM), for the help in the modeling work and Nur Bahiyah for her help in translation of the abstract.

I would like to gratefully acknowledge Universiti Sains Malaysia (USM) Postgraduate Research Grant Scheme (USM-RU-PRGS), 1001/PKIMIA/841008 and a USM Research University Fellowship scheme for the financial support. I am truly

grateful to all members of the School of Chemical Sciences who were always willing to help.

I would like to express my deepest appreciation to my friends in HIKMA Pharmaceuticals Company, Amman-Jordan for providing me with the working standards.

I would also like to extend my thanks to my roommates and friends Ahmad Makahleh, Abdassalam Tameem, Mohammad Talaq, Marwan Shalash and Mr. Ariffin and who made my stay at USM a very memorable one.

Last but not least, I would like to thank my family members (mother, sisters, brothers, nieces, nephews and relatives) for their love, prayers, support, their lasting encouragement, making me smile, and inspired me in a way no one else could. My mother has always motivated me to achieve greater success throughout my academic career and it is to them that I dedicate this thesis. This would not have been possible without them.

Specially dedicated to:

My late Dad,

My mum,

Brothers & sisters,

Niece & nephews

My relatives and friends

TABLE OF CONTENTS

	Page
Acknowledgments	ii
Table of Contents	v
List of Tables	xiv
List of Figures	xvi
List of Abbreviations	xxi
Abstrak	xxviii
Abstract	xxx
CHAPTER 1: INTRODUCTION	1
1.1 Capillary Electrophoresis	1
1.2 Theory of Electrophoretic Separation	3
1.3 Chirality	6
1.4 Analytical Methods for the Analysis of Chiral Compounds	10
1.5 Chiral Separation Modes	13
1.6 Chiral Selectors	17
1.6.1 Proteins	18
1.6.2 Polysaccharides	19
1.6.3 Macrocyclic Antibiotics	22
1.6.4 Ligand Exchangers	23
1.6.5 Cyclodextrins	25
1.7 Recent Developments in Capillary Electrophoresis	28
1.7.1 Detectors	29
1.7.2 CE at the Omics Level	31
1.7.3 Green Sample Preparation Techniques and Automation	32
1.7.4 Portable CE	35
1.7.5 Microfluidics	36

1.7.6 Chiral Monolithic Stationary Phases in CEC 37

1.7.7 Analysis of Microbes 41

1.8 Objectives 42

CHAPTER 2: SIMULTANEOUS DETERMINATION OF THE β-BLOCKER DRUG (ATENOLOL), DIURETIC (CHLORTHALIDONE AND AMILORIDE) IN PHARMACEUTICAL PREPARATIONS BY CZE WITH ULTRAVIOLET AND CAPACITIVELY COUPLED CONTACTLESS CONDUCTIVITY DETECTIONS 44

2.1 Introduction 44

2.2 CZE Method Development for the Determination of Atenolol, Chlorthalidone and Amiloride Using UV Detection 46

2.2.1 Experimental 49

2.2.1.1 Chemicals and Reagents 49

2.2.1.2 Instrumentation and Electrophoretic Conditions .. 49

2.2.1.3 Preparation of Standard Solutions 50

2.2.1.4 Pharmaceutical Sample Preparation 50

2.2.2 Results and Discussion 51

2.2.2.1 Optimization of Separation Conditions 51

2.2.2.1(a) Effect of Buffer pH 51

2.2.2.1(b) Effect of Buffer Concentration 51

2.2.2.1(c) Effect of Applied Voltage 52

2.2.2.1(d) Effect of Capillary Temperature ... 52

2.2.2.1(e) Effect of Injection Time 53

2.2.2.2 Validation of the Analytical Method 54

2.2.2.2(a) Calibration Curve, Limits of Detection and Quantitation 54

2.2.2.2(b) Precision 54

2.2.2.2(c) Accuracy 55

2.2.2.3 Analysis of Pharmaceutical Formulations 56

2.2.3 Conclusions 56

2.3 CZE Method Development for the Determination of Atenolol and Amiloride Using C^4D Detection 59

2.3.1 Experimental 61

2.3.1.1 Chemicals and Reagents 61

2.3.1.2 Instrumentation and Electrophoretic Conditions . 61

2.3.1.3 Preparation of Standard Solutions 62

2.3.1.4 Pharmaceutical Sample Preparation 62

2.3.2 Results and Discussion 63

2.3.2.1 Optimization of Separation Conditions 63

2.3.2.1(a) BGE Selection 63

2.3.2.1(b) Effect of the Buffer Concentration . 64

2.3.2.1(c) Effect of C^4D Detector Excitation Voltage and Frequency 64

2.3.2.1(d) Effect of Applied Voltage 64

2.3.2.1(e) Effect of Capillary Temperature .. 65

2.3.2.1(f) Effect of Injection Time 65

2.3.2.2 Validation of the Analytical Method 66

2.3.2.2(a) Calibration Curve, Limits of Detection and Quantitation 66

2.3.2.2(b) Precision 67

2.3.2.2(c) Accuracy 68

2.3.2.3 Analysis of Pharmaceutical Formulations 69

2.3.3 Conclusions 71

CHAPTER 3: SIMULTANEOUS DETERMINATION OF VALACYCLOVIR, ACYCLOVIR AND THEIR MAJOR IMPURITY (GUANINE) IN PHARMACEUTICAL FORMULATIONS USING MEKC METHOD 72

3.1 Introduction 72

3.2 Method Development Based on MEKC 74

3.2.1 Experimental 78

3.2.1.1 Chemicals and Reagents 78

3.2.1.2 Instrumentation and Electrophoretic Conditions 78

3.2.1.3 Preparation of Standard Solutions 79

3.2.1.4 Pharmaceutical Sample Preparation 79

3.2.1.5 Preparation of Placebos 80

3.2.2 Results and Discussion 81

3.2.2.1 Optimization of Separation Conditions 81

3.2.2.1(a) Effect of Buffer pH 81

3.2.2.1(b) Effect of Surfactant Concentration . 83

3.2.2.1(c) Effect of Buffer Concentration 84

3.2.2.1(d) Effect of Injection Time 85

3.2.2.1(e) Effect of Applied Voltage 85

3.2.2.1(f) Effect of Capillary Temperature ... 86

3.2.2.2 Validation of the Analytical Method 87

3.2.2.2(a) Calibration Curve, Limits of Detection and Quantitation 87

3.2.2.2(b) Precision 89

3.2.2.2(c) Accuracy 90

3.2.2.2(d) Specificity 92

3.2.2.3 Analysis of Pharmaceutical and Cream Formulations 93

3.2.3 Conclusions 96

CHAPTER 4: ENANTIOSELECTIVE ANALYSIS OF OFLOXACIN AND ORNIDAZOLE IN PHARMACEUTICAL FORMULATIONS BY CZE: METHOD

DEVELOPMENT AND COMPUTATIONAL MODELING OF THEIR INCLUSION COMPLEXES . . 97

4.1 Introduction 97

4.2 Method Development for the Simultaneous Chiral Separation of Ofloxacin and Ornidazole 99

4.2.1 Experimental 101

4.2.1.1 Chemicals and Reagents 101

4.2.1.2 Instrumentation and Electrophoretic Conditions . 101

4.2.1.3 Stock and Standard Solutions 102

4.2.1.4 Pharmaceutical Sample Preparation 103

4.2.2 Results and Discussion 103

4.2.2.1 Optimization of Separation Conditions 103

4.2.2.1(a) Effect of Buffer pH 103

4.2.2.1(b) Effect of Buffer Concentration 105

4.2.2.1(c) Effect of Chiral Selector Concentration 105

4.2.2.1(d) Effect of Applied Voltage 107

4.2.2.1(e) Effect of Injection Time 107

4.2.2.1(f) Effect of Capillary Temperature 107

4.2.2.2 Validation of the Analytical Method 109

4.2.2.2(a) Calibration Curve, Limits of Detection and Quantitation 109

4.2.2.2(b) Precision 110

4.2.2.2(c) Accuracy 112

4.2.2.2(d) Selectivity 112

4.2.2.3 Analysis of Pharmaceutical Formulation 112

4.2.3 Conclusions 113

4.3 Computer Modeling of Ofloxacin-Cyclodextrin and Ornidazole- Cyclodextrin Complexes 114

4.3.1 Experimental 114

4.3.2 Results and Discussion 115

4.3.3 Conclusions 120

CHAPTER 5: ENANTIOSEPARATION OF MODAFINIL AND ITS ENANTIOMERS BY CZE: METHOD DEVELOPMENTS, COMPUTATIONAL MODELING AND BINDING CONSTANTS MEASUREMENTS OF THE RELEVANT HOST-GUEST COMPLEXES 121

5.1 Introduction 121

5.2 Method Development for the CZE Determination of Achiral Modafinil 123

5.2.1 Experimental 124

5.2.1.1 Chemicals and Reagents 124

5.2.1.2 Instrumentation 124

5.2.1.3 Electrophoretic Conditions 125

5.2.1.4 Stock and Standard Solutions 125

5.2.1.5 Pharmaceutical Sample Preparation 125

5.2.2 Results and Discussion 127

5.2.2.1 Optimization of Separation Conditions 127

5.2.2.1(a) Effect of Buffer pH 127

5.2.2.1(b) Effect of Buffer Concentration 128

5.2.2.1(c) Effect of Applied Voltage 129

5.2.2.1(d) Effect of Injection Time 129

5.2.2.1(e) Effect of Capillary Temperature ... 129

5.2.2.2 Validation of the Analytical Methods 131

5.2.2.2(a) Calibration Curve, Limits of Detection and Quantitation 131

5.2.2.2(b) Precision 132

5.2.2.2(c) Accuracy 134

5.2.2.2(d) Robustness 134

5.2.2.3 Stress Testing and Specificity 135

5.2.2.4 Analysis of Pharmaceutical Formulation 135

5.2.3 Conclusions 136

5.3 Method Development for the Chiral Separation of Modafinil 137

5.3.1 Experimental 137

5.3.1.1 Chemicals and Reagents 137

5.3.1.2 Instrumentation 137

5.3.1.3 Electrophoretic Conditions 138

5.3.1.4 Stock and Standard Solutions 138

5.3.1.5 Pharmaceutical Sample Preparation 138

5.3.2 Results and Discussion 139

5.3.2.1 Optimization of Separation Conditions 139

5.3.2.1(a) Effect of Buffer pH 139

5.3.2.1(b) Effect of Buffer Concentration 140

5.3.2.1(c) Effect of Chiral Selector Concentration 141

5.3.2.1(d) Effect of Applied Voltage 142

5.3.2.1(e) Effect of Injection Time 143

5.3.2.1(f) Effect of Capillary Temperature 144

5.3.2.2 Validation of the Analytical Method 145

5.3.2.3 Analysis of Pharmaceutical Formulation 147

5.3.3 Conclusions 147

5.4 Computer Modeling of Modafinil-Cyclodextrin Complexes 148

5.4.1 Experimental 149

5.4.2 Results and Discussion 150

5.4.3 Conclusions 155

5.5 Binding Constants Measurements of Modafinil-Cyclodextrin Complexes 156

5.5.1 Experimental 157

5.5.2 Results and Discussion 158

5.5.2.1 Determination of Binding Constants 158

5.5.2.2 Determination of Thermodynamic Parameters ... 168

5.5.3 Conclusions 171

CHAPTER 6: CZE TECHNIQUE FOR THE TRACE DETERMINATION OF ROSIGLITAZONE (ANTI DIABETIC DRUG) IN BIOLOGICAL FLUIDS PRECEDED BY THREE PHASE HOLLOW FIBER LIQUID PHASE MICROEXTRACTION 172

6.1 Introduction 172

6.2 Method Development for the CZE Determination of Rosiglitazone 173

6.2.1 Experimental 175

6.2.1.1 Chemicals and Reagents 175

6.2.1.2 Instrumentation and Electrophoretic Conditions 176

6.2.1.3 Standard Solutions and Real Samples 177

6.2.1.4 HF-LPME Procedure 177

6.2.1.5 Minimizing Protein Binding in Plasma 179

6.2.1.6 Minimizing Matrix Effects in Urine 180

6.2.2 Results and Discussion 180

6.2.2.1 Optimization Conditions for HF-LPME 181

6.2.2.1(a) Selection of Organic Solvent 181

6.2.2.1(b) Effect of Donor Phase pH 182

6.2.2.1(c) Effect of Acceptor Phase Concentration 184

6.2.2.1(d) Effect of Stirring Speed 184

6.2.2.1(e) Effect of Extraction Time 185

6.2.2.1(f) Effect of Salt Addition 186

6.2.2.1(g) Adopted Extraction Conditions ... 187

6.2.2.2 Method Validation 188

6.2.2.3 Comparison with Previously Reported Methods . 188

6.2.2.4 Extraction of Rosiglitazone from Real Samples . 190

6.2.3 Conclusions 191

CHAPTER 7: CONCLUDING REMARKS AND SUGGESTIONS FOR FUTURE STUDIES 193

7.1 Concluding Remarks 193

7.2 Suggestions for Future Studies 195

REFERENCES 196

LIST OF PUBLICATIONS AND PRESENTATIONS AT CONFERENCES 225

LIST OF TABLES

		Page
Table 1.1	The main properties of native cyclodextrins (Fanali, 2000)	25
Table 1.2	Commercial native cyclodextrins and derivatives (Subramanian, 2007)	28
Table 1.3	Applications of organic monoliths (Smith and Jiang, 2008)	40
Table 2.1	Intra and inter-day precision for the determination of atenolol (AT), amiloride (AM) and chlorthalidone (CH)	55
Table 2.2	Accuracy results for the determination atenolol (AT), amiloride (AM) and chlorthalidone (CH) spiked to tablet	56
Table 2.3	Assay results of atenolol (AT), amiloride (AM) and chlorthalidone (CH) in different pharmaceutical formulations	58
Table 2.4	Intra- and inter-day precision for the determination of atenolol (AT) and amiloride (AM)	68
Table 2.5	Accuracy results for the determination atenolol (AT) and amiloride (AM) spiked to tablet	68
Table 2.6	Assay results of atenolol (AT) and amiloride (AM) in different pharmaceutical formulations	70
Table 3.1	Adopted CZE operating conditions	87
Table 3.2	Within day and inter-day repeatability for the repeated injections of different mixtures of VCV, ACV and guanine standard solutions	89
Table 3.3	Accuracy of the MEKC method	91
Table 3.4	Results form the determination of the active ingredients and guanine in pharmaceutical and cream formulations	94
Table 4.1	Adopted CZE operating conditions	108
Table 4.2	Within-day and inter-day reproducibility for the repeated introductions of different concentrations of racemic ofloxacin and ornidazole standards	111
Table 4.3	Recoveries obtained from the determination of ofloxacin and ornidazole when spiked with different levels of standards	112
Table 4.4	Results for the determination of enantiomers of ofloxacin and ornidazole in co- formulated tablets	113

Table 4.5	Relative energies of the lowest energy conformations for the ornidazole and ofloxacin enantiomers inclusion complexes with S-β-CD calculated at PM3 level. All energies are in kJ mol^{-1}	115
Table 5.1	Repeatability of various parameters expressed as % RSD	133
Table 5.2	Intra and inter-assay precision for modafinil (6 days)	133
Table 5.3	Determination modafinil sample under different conditions using the CZE method (n = 6)	134
Table 5.4	Results for the determination of modafinil when subjected to different stressed conditions*	135
Table 5.5	Adopted CZE operating conditions	144
Table 5.6	Intra-day and inter-day reproducibility for the repeated injection of different concentrations of racemic modafinil standards	146
Table 5.7	Recovery values obtained from the determination of modafinil when spiked with different levels of standards	146
Table 5.8	PM3 calculated total energy and energy of complexation of modafinil enantiomers with β-CD and S-β-CD	151
Table 5.9	Binding constant (M^{-1}) between modafinil enantiomers with S-β-CD at different temperatures	166
Table 6.1	Comparison of the newly developed method with other reported methods for the determination of rosiglitazone (ROSI)	189
Table 6.2	Results for the determination of rosiglitazone (ROSI) in spiked samples subjected to the HF-LPME and analyzed using CZE	190

LIST OF FIGURES

		Page
Figure 1.1	Schematic diagram of a CE instrumental set-up	1
Figure 1.2	A model of a double electric layer on the interface of a silica capillary with aqueous buffer (A) and zeta potential (ζ) of the system as a function of the distance away from the wall (B) (Salomon *et al.*, 1991)	5
Figure 1.3	Chemical structure of the chiral limonene, (*R*)-Limonene smells of oranges and (*S*)-limonene smells of lemons (Ahlberg, 2001)	7
Figure 1.4	Chemical structures of a few chiral drugs having different effects (Johannsen, 2001; Awadallah *et al.*, 2003; Behn *et al.*, 2001)	9
Figure 1.5	Chemical structures of several stereochemically pure drugs as single enantiomers patented in the last few years (Maier *et al.*, 2001)	11
Figure 1.6	Number of CE publications since 1985. Search engine, Scopus, search keywords, "capillary electrophoresis and chiral" and "capillary electrophoresis".	12
Figure 1.7	Scheme of migration modes in CE for chiral molecules (Subramaian, 2007)	14
Figure 1.8	Chemical structures of some polysaccharides used as chiral selectors	20
Figure 1.9	Possible structures for the ternary complexes formed between the enantiomers of 3-phenyl-lactic acid and L-hydroxyproline (Blanco and Valverde, 2003)	24
Figure 1.10	(A) Chemical structure of β-cyclodextrin and (B) its cup-shaped	26
Figure 1.11	Number of papers that used CE for the analysis of different analytes that appeared in "PubMed) database from January 2008 to June 2009 (Oh *et al.*, 2010)	32
Figure 1.12	Sample-preparation methods that can be applied with CE. HF, Hollow fibre; LLE, Liquid-liquid extraction; LPME, Liquid-phase microextraction; MD, Microdialysis; SFE, Supercritical fluid extraction; SLM, Supported liquid membrane; SPE, Solid-phase extraction, SPME, Solid-phase microextraction (Arce *et al.*, 2009)	33

Figure 1.13	On-line, at-line and in-line combinations of liquid-phase microextraction coupled to CE (LPME-CE) (Arce *et al.*, 2009)	34
Figure 1.14	Commercial portable capillary electrophoresis design with UV detector (Ryvolová *et al.*, 2010)	35
Figure 1.15	Schematic diagram of a miniaturized CE system with automated continuous sample introduction system (Xu *et al.*, 2009)	37
Figure 2.1	Chemical structures of the drugs and internal standards (IS) used in the studies	48
Figure 2.2	Typical electropherograms obtained when operated under the adopted conditions using UV detection. (A) 100 μg mL^{-1} standard, (B) Teklo tablet. 1- atenolol, 2- amiloride, 3- chlorthalidone, and 4- Internal standard (phenobarbital). Conditions: 25 mM H_3PO_4 adjusted with 1 M NaOH, pH 9.0, voltage, 25 kV; temperature, 25 °C; and injection time, 10 s	53
Figure 2.3	Axial capacitively coupled contactless conductivity detector for CZE (Kubáň and Hauser, 2009)	60
Figure 2.4	Typical electropherograms obtained when operated under the adopted conditions using C^4D detection. (A) 150 μg mL^{-1} standard, (B) Teklo tablet. 1- amiloride, 2- atenolol, and 3- Internal standard (L-valine). Conditions: 150 mM acetic acid, voltage, 25 kV; temperature, 28 °C; injection time, 25 s; and detector excitation signal of 100 V and 350 kHz	66
Figure 3.1	Chemical structures of the drugs and internal standard (IS) used in the studies	73
Figure 3.2	Bioconversion pathway of valacyclovir (Stella *et al.*, 2007)	74
Figure 3.3	Schematic illustration of the separation principle of MEKC (Gübitz and Schmid, 2004)	75
Figure 3.4	Effect of pH on the migration time of analytes (buffer concentration, 20 mM citric acid- adjusted with 1 M tris; SDS concentration, 125 mM; temperature, 28 °C; and applied voltage, 25 kV, reversed polarity)	82
Figure 3.5	Effect of SDS concentration on the migration of VCV, ACV and guanine (20 mM citric acid- adjusted with 1 M tris solution; pH 2.75; temperature 28 °C, and applied voltage, 25 kV)	84
Figure 3.6	Electropherogram obtained from the introduction of standard mixture containing VCV, ACV, guanine and tyramine (internal standard) to show the separation between the analytes, operated under the adopted conditions. Peaks, (1): VCV, (2): internal	86

standard, (3): guanine and (4): ACV. Please refer to Table 3.1 for CZE conditions

Figure 3.7 Electropherogram obtained from the introduction of different placebos forms. (A): Tablet placebo; (B): ACV cream (chlorocresol as preservative) placebo; (C): ACV cream (methyl paraben & propyl paraben as preservatives) placebo. Please refer to Table 3.1 for CZE conditions 92

Figure 3.8 Electropherograms obtained from the analysis of commercial formulations. (A): VCV tablet (sample # 1); (B): ACV tablet (sample # 5); (C): ACV cream containing chlorocresol as preservatives (sample # 9); (D): Acyclovir cream containing methyl paraben & propyl paraben placebo (sample # 10). Peaks: (1): VCV; (2): Tyramine IS; (3): Guanine; (4): ACV; (5): unidentified peaks from placebo. Please refer to Table 3.1 for CZE conditions 95

Figure 4.1 Chemical structures of ofloxacin and ornidazole, the asterisks indicate the chiral centers 98

Figure 4.2 Effect of pH on the resolution of ofloxacin and ornidazole enantiomers (buffer concentration, 50 mM H_3PO_4- adjusted with 1 M tris; S-β-CD concentration, 30 mg mL^{-1}; temperature, 25 °C; and applied voltage, 18 kV; reversed polarity) 104

Figure 4.3 Effect of S-β-CD concentration on the resolution of ofloxacin and ornidazole enantiomers (50 mM H_3PO_4- adjusted with 1 M tris solution; pH 1.85; temperature 25 °C, and applied voltage, 18 kV; reversed polarity) 106

Figure 4.4 Electropherograms obtained from the injection of racemic ofloxacin and ornidazole standards (A); and tablet (B). Please refer to Table 4.1 for CZE conditions 109

Figure 4.5 The side and top views of the lowest energy conformations obtained from PM3 calculations for (a); *R*-ornidazole/S-β-CD and (b); *S*-ornidazole/S-β-CD complexes 116

Figure 4.6 The side and top views of the lowest energy conformations obtained from PM3 calculations for (a); *R*-ofloxacin/ S-β-CD and (b); *S*-ofloxacin S-β-CD complexes 117

Figure 5.1 Chemical structure of modafinil, the asterisk indicates the chiral center 122

Figure 5.2 Effect of buffer pH on: (A) migration time, (B) peak width. 20 mM H_3PO_4- adjusted with 1 M tris, pH 9.0 buffer solution, voltage: 25 kV, temperature: 25 °C, and injection time: 5 s 127

Figure 5.3	Electropherograms of (A) modafinil standard, upon heating at 75 °C for 15 h. (B) modafinil standard, containing 1M HCl, heated at 75 °C for 15 h. (C) modafinil standard, containing 1M NaOH, heated at 75 °C for 15 h. (D) modafinil standard, containing 30 % H_2O_2, heated at 75 °C for 15 h. 1- modafinil, 2-Internal standard (phenobarbital). Conditions: 20 mM H_3PO_4- adjusted with 1 M tris, pH 9.0, voltage: 25 kV, temperature: 25 °C, and injection time: 5 s	131
Figure 5.4	Typical electropherograms obtained when operated under the adopted conditions. (A) (250 μg $mL^{-1}$of standard), (B) modafinil tablet. 1-modafinil, 2-internal standard (phenobarbital). Conditions: 20 mM H_3PO_4- adjusted with 1 M tris, pH 9.0, voltage: 25 kV, temperature: 25 °C, and injection time: 5 s	136
Figure 5.5	Effect of pH on the resolution of modafinil enantiomers (buffer concentration, 25 mM H_3PO_4- adjusted with 1 M tris; S-β-CD concentration, 30 mg mL^{-1}; temperature, 25 °C; and applied voltage, 18 kV)	140
Figure 5.6	Effect of S-β-CD concentration on the resolution of modafinil enantiomers (25 mM H_3PO_4- adjusted with 1 M tris solution; pH 8.0; temperature 25 °C, and applied voltage, 18 kV)	142
Figure 5.7	Electropherogram obtained from the injection of racemic modafinil standard (A); and tablet (B). Please refer to Table 5.5 for CZE conditions	145
Figure 5.8	Energy minimized structures obtained from PM3 calculations for the (a) *S*-modafinil/β-CD complexes seen from the side wall of β-CD (b) *S*-modafinil/β-CD complexes seen from the secondary hydroxyl rim of the β-CD cavity (c) *R*-modafinil/β-CD complexes seen from the side wall of β-CD (d) *R*-modafinil/β-CD complexes seen from the secondary hydroxyl rim of the β-CD cavity	152
Figure 5.9	Energy minimized structures obtained from PM3 calculations for the (a) *S*-modafinil/S-β-CD complexes seen from the side wall of S-β-CD (b) *S*-modafinil/S-β-CD complexes seen from the secondary hydroxyl rim of the S-β-CD cavity (c) *R*-modafinil/S-β-CD complexes seen from the side wall of S-β-CD (d) *R*-modafinil/S-β-CD complexes seen from the secondary hydroxyl rim of the S-β-CD cavity	153
Figure 5.10	Electropherograms obtained from the injection of racemic modafinil standard under the adopted CZE conditions. Please refer to Table 5.5 for CZE conditions	160

Figure 5.11	Change in modafinil enantiomers mobility versus S-β-CD concentration at different temperatures	164
Figure 5.12	Van't Hoff plot for modafinil enantiomer-S-β-CD complexes	169
Figure 6.1	Chemical structure of rosiglitazone (ROSI) maleate. pK_a values (6.1 and 6.8), log K_{ow} (2.56) (Yardimci and Özaltin, 2005)	173
Figure 6.2	Schematic diagram of HF-LPME set-up	179
Figure 6.3	Effects of organic solvent on the enrichment factor (n = 3). Experimental conditions: donor phase volume, 10 mL; acceptor phase 15 µL (0.1 M HCl); concentration level, 500 ng mL^{-1}; pH, 8.5; extraction time, 15 min; and stirring speed, 300 rpm	182
Figure 6.4	Effects of donor pH on enrichment factor (n = 3). Experimental conditions are as follow: organic solvent, dihexyl ether; donor phase volume, 10 mL; acceptor phase 15 µL (0.1 M HCl); concentration level, 500 ng mL^{-1}; extraction time, 15 min; and stirring speed, 300 rpm	183
Figure 6.5	Effects of stirring speed on enrichment factor (n = 3). Experimental conditions are as follow: organic solvent, dihexyl ether; donor phase, 10 mL (pH, 9.5); acceptor phase, 15 µL (0.1 M HCl); concentration level, 500 ng mL^{-1}; and extraction time, 15 min	185
Figure 6.6	Effects of extraction time on the enrichment factor (n = 3). Experimental conditions are as follow: organic solvent, dihexyl ether; donor phase, 10 mL (pH, 9.5); acceptor phase, 15 µL (0.1 M HCl); concentration level, 500 ng mL^{-1}; and stirring speed, 600 rpm	186
Figure 6.7	Effects of salt addition on the enrichment factor (n = 3). Experimental conditions are as follow: organic solvent, dihexyl ether; donor phase, 10 mL (pH, 9.5); acceptor phase, 15 µL (0.1 M HCl); concentration level, 500 ng mL^{-1}; stirring speed, 600 rpm and extraction time, 30 min	187
Figure 6.8	Electropherograms of samples subjected to the HF-LPME and analysed using the CZE-UV method. (A) plasma, (B) spiked plasma, (C) urine and (D) spiked urine. Plasma and urine samples were diluted 1:4 and 1:1 (sample:water), respectively. Spiked samples refer to samples that had been spiked with 10 ng mL^{-1} ROSI. Please see the optimized HF-LPME conditions in addition to the CZE conditions under sections 6.2.2.1(g) and 6.2.1.2, respectively	191

LIST OF ABBREVIATIONS

T	Absolute temperature
pK_a	Acid dissociation constant
AP	Acceptor phase
ACV	Acyclovir
AM	Amiloride hydrochloride
r	Analyte radius
Å	Angstrom
μ_a	Apparent mobility
E	Applied electric field
V	Applied voltage
μ_{av}	Arithmetic mean of mobilities
AT	Atenolol
BGE	Background electrolyte
K	Binding constant
K_S	Binding constant for the *S* enantiomer
K_R	Binding constant for the *R* enantiomer
BSA	Bovine serum albumin
CSD	Cambridge structural database
C^4D	Capacitively coupled contacless conductivity detection
CAE	Capillary array electrophoresis
CE	Capillary electrophoresis
CEC	Capillary electrochromatography
CZE	Capillary zone electrophoresis
cm	Centimemter
q	Charge of molecule
CH	Chlorthalidone

μ_{Cor}	Corrected electrophoretic mobility
C_a	Concentration of analyte in the organic phase after extraction
C_{AP}	Concentration of analyte in the acceptor phase
CD	Cyclodextrin
α-CD	Alpha cycodextrin
β-CD	Beat cyclodextrin
γ-CD	Gama cyclodextrin
CM-β-CD	Carboxymethyl-β-cyclodextrin
CMC	Critical micelle concentration
DNA	Deoxyribonucleic acid
ε	Dielectric constant
D	Diffusion coefficient
ΔE_{R-S}	Difference in energies between the diastereoisomeric complexes
DP	Donor phase
l	Effective capillary length
ECD	Electrochemical detection
EOF	Electroosmotic flow
μ_{EOF}	Electroosmotic flow mobility
μ_f	Electrophoretic mobility of the free analyte
μ_c	Electrophoretic mobility of the complexed analyte
$\Delta\mu$	Electrophoretic mobility difference of the analytes
α	Enantioselectivities of complexation
EF	Enrichment factor
$\Delta H°$	Enthalpy change
$\Delta\Delta H°$	Enthalpy difference
$\Delta S°$	Entropy change
$\Delta\Delta S°$	Entropy difference
[C]	Equilibrium concentration of the uncomplexed ligand

EP	European Pharmacopeia
ER	Extraction recovery
FDA	Food and Drug Administration
GC	Gas chromatography
R	Gas constant
ΔG°	Gibbs free energy
$\Delta\Delta G^{\circ}$	Gibbs free energy difference
g	Gram
DM-β-CD	Heptakis-2,6-dimethyl-β-cyclodextrin
TM-β-CD	Heptakis-2,3,6-trimethyl-β-cyclodextrin
HS-β-CD	Heptakis-6-sulfo-β-cyclodextrin
HDAS-β-CD	Heptakis-(2,3-diacetyl-6-sulfo)-β-cyclodextrin
HSV	Herpes simplex virus
Hz	Hertz
HPLC	High performance liquid chromatography
HF	Hollow fibre
h	Hour
HP-α-CD	Hydroxypropyl-α-cyclodextrin
HP-β-CD	Hydroxypropyl-β-cyclodextrin
HP-γ-CD	Hydroxypropyl-γ-cyclodextrin
TMA-β-CD	2-hydroxy-3-trimethylammoniopropyl-β-cyclodextrin
C_0	Initial concentration of analyte in the source phase
C_d	Initial concentration of analyte in the sample solution before extraction
I.D	Internal diameter
IS	Internal standard
T_{iso}	Isoenantioselective temperature
KHz	Kilohertz

kcal mol^{-1}	Kilocalories per mole
kJ mol^{-1}	Kilojoules per mole
kV	Kilovolt
LIF	Laser induced fluorescence
LC	Liquid chromatography
LOD	Limit of detection
LOQ	Limit of quantitation
LLE	Liquid-liquid extraction
LPME	Liquid-phase microextraction
log K_{ow}	Log octanol-water partitioning coefficient
MS	Mass spectrometry
λ_{max}	Maximum wavelength
M-α-CD	Methyl-α-cyclodextrin
M-β-CD	Methyl-β-cyclodextrin
MP	Methyl paraben
µA	Microampere
MD	Microdialysis
min	Minute
MEKC	Micellar electrokinetic chromatography
µg	Microgram
µL	Microliter
µm	Micrometer
µCE	Microchip capillary electrophoresis
t_R	Migration time
mbar	Millibar
mg	Milligram
mL	Millilitre
mmol	Millimole

mM	Millimolar
mm Hg	Millimeters of mercury
mW	Milliwatt
mW/m	Milliwatt per meter
ME-1	Modafinil enantiomer 1
ME-2	Modafinil enantiomer 2
M	Molar
mol	Mole
MIP	Molecularly imprinted polymer
ng	Nanogram
nL	Nanoliter
nm	Nanometer
N/D	Not detected
N/A	Not applicable
μ_{Obs}	Observed electrophoretic mobility
OF-E1	Ofloxacin enantiomer 1
OF-E2	Ofloxacin enantiomer 2
$[C]_{opt}$	Optimal CD concentration
OR-E1	Ornidazole enantiomer 1
OR-E2	Ornidazole enantiomer 2
W	Peak width
%	Percentage
PDA	Photo diode array
pg	Picogram
pL	Picoliter
PP	Propyl paraben
rpm	Rate per minute
rcf	Relative centrifugal force

r^2	Regression coefficient
RSD	Relative standard deviation
R_s	Resolution
RNA	Ribonucleic acid
ROSI	Rosiglitazone
s	Second
S/N	Signal-to-noise ratio
SDS	Sodium dodecyl sulfate
SPE	Solid-phase extraction
SPME	Solid-phase microextraction
SD	Standard deviation
SFE	Supercritical fluid extraction
SLM	Supported liquid membrane
S-α-CD	Sulfated α-cyclodextrin
S-β-CD	Sulfated β-cyclodextrin
S-γ-CD	Sulfated γ-cyclodextrin
SB-β-CD	Sulfobutyl-β-cyclodextrin
°C	Temperature in degree Celsius
IUPAC	The International Union of Pure and Applied Chemistry
N	Theoretical plates
L	Total capillary length
E_{fg}	Total energy of the free guest molecule
$E_{\beta CD}$	Total energy of the free host molecule for beta cyclodextrin
$E_{S\text{-}\beta CD}$	Total energy of the free host molecule for sulfated beta cyclodextrin
ΔE_{comp}	Total complexation energy of the host-guest
UV	Ultraviolet detection
USP	United States Pharmacopeia
VCV	Valacyclovir

v	Velocity of the charged analyte
η	Viscosity
η_o	Viscosity of the solution without chiral selector
η_x	Viscosity of the solution at specific chiral selector concentration
V_{AP}	Volume of acceptor phase
V_{DP}	Volume of donor phase
W/m	Watt per meter
ζ	Zeta potential

PERKEMBANGAN KAEDAH ANALISIS DAN KAJIAN ASAS PEMISAHAN DADAH MENGGUNAKAN ELEKTROFORESIS RERAMBUT

ABSTRAK

Kaedah electrophoresis zon rerambut (CZE) bagi pemisahan serentak dadah β-sekatan (atenolol (AT), klortalidon (CH) dan amilorid (AM)), menggunakan pengesan UV dan kekonduksian tanpasentuh kupel kapasitif (C^4D) telah diperkembangkan dan divalidasikan. Bagi keadaan yang digunakan, analit telah dipisahkan kurang daripada 4 min dan 7 min masing-masing bagi kaedah CZE-UV dan CZE-C^4D. Kaedah CZE-C^4D mempunyai kepekaan yang rendah, tetapi kedua kaedah telah diaplikasikan dengan jayanya bagi penentuan bahan aktif di dalam sediaan farmaseutik.

Satu kaedah kromatografi elektrokinetik misel bagi penentuan serentak dadah antiviral acyclovir (ACV) dan valacyclovir (VCV) dan bendasing utama (guanina) telah diperkembangkan. Bagi keadaan yang digunakan (BGE 20 mM asid sitrik dilaraskan dengan larutan tris 1 M (pH 2.75) mengandungi 125 mM natrium dodesil sulfat) dan semua analit telah dipisahkan dalam masa 4 min.

Satu kaedah CZE bagi pemisahan serentak enantiomer oflosaksin dan ornidazol menggunakan β-siklodekstrin-sulfat (S-β-CD) sebagai pemilih kiral juga dihuraikan. Masa analisis yang baik (kurang daripada 16 min) dengan resolusi masing-masing 5.45 dan 6.28 bagi enantiomer oflosaksin dan ornidazol, telah dicapai menggunakan BGE 50 mM H_3PO_4 dilaraskan dengan 1 M larutan tris; pH 1.85; mengandungi 30 mg mL^{-1} S-β-CD. Perolehan semula antara 97.1 – 104.0 % telah diperolehi.

Perkiraan komputasional bagi kompleks rangkuman enantiomer telah juga dihuraikan.

Satu kaedah CZE mudah penunjuk kestabilan bagi penentuan modafinil dalam formulasi farmaseutik telah diperkembangkan. Kaedah menunjukkan bukan sahaja kepresisan dan kejituan yang baik tetapi juga "robust" yang baik. LOQ dan LOD masing-masing adalah 1.2 dan 3.5 $\mu g\ mL^{-1}$. Eksipien di dalam tablet dan hasil peruraian dari keadaan berbeza tertekan tidak mengganggu dalam penentuan.

Satu kaedah pantas CZE telah juga diperkembangkan dan divalidasikan bagi penentuan enantiomer modafinil dalam kurang daripada 5 min dengan resolusi yang baik (Rs = 2.51) menggunakan BGE 25 mM H_3PO_4 dilaraskan dengan larutan 1 M tris; pH 8.0; mengandungi 30 mg mL^{-1} S-β-CD. Perkiraan komputasional, menyukatan pemalar penambatan (plot resiprokal dubel, resiprokal-*X* dan resiprokal-*Y*) dan juga parameter termodinamik telah juga dijalankan. Semua kaedah yang diperkembangkan di atas telah divalidasikan, dan telah di aplikasikan dengan jayanya bagi penentuan analit di dalam formulasi farmaseutikal.

Satu mikropengekstrakan fasa cecair serabut / gentian rongga fasa-tiga (HF-LPME) diikuti dengan pemisahan CZE telah diperkembangkan dengan jayanya dan divalidasikan bagi penentuan paras surihan dadah antidiabetik rosiglitazon (ROSI) dalam cecair biologi. Bagi keadaan yang dioptimumkan (pelarut pengekstrakan, diheksil eter; pH fasa penderma, 9.5; fasa penerima, 0.1M HCl; halaju pengacauan, 600 rpm; masa pengekstrakan, 30 min; tanpa campuran garam), faktor mengkayaan 280 telah dicapai. Kelinearan baik dan pemalar korelasi analit telah dicapai bagi julat kepekatan 5.0 - 500 ng mL^{-1} (r^2 = 0.9967). Kaedah ini adalah ringkas, peka dan sesuai bagi penentuan amaun surih ROSI di dalam cecair biologi.

ANALYTICAL METHOD DEVELOPMENT AND FUNDAMENTAL STUDIES ON THE SEPARATION OF DRUGS USING CAPILLARY ELECTROPHORESIS

ABSTRACT

Capillary zone electrophoresis (CZE) methods for the simultaneous separation of the β-blocker drugs (atenolol (AT), chlorthalidone (CH) and amiloride (AM)), using UV and capacitively coupled contactless conductivity detectors (C^4D) were developed and validated. Under the adopted conditions, the analytes were separated in less than 4 min and 7 min for the CZE-UV and the CZE-C^4D methods, respectively. The CZE-C^4D method has slightly inferior sensitivity, but nevertheless, both methods were successfully applied to the determination of the active ingredients in pharmaceutical preparations.

A micellar electrokinetic chromatography (MEKC) method for the simultaneous determination of the antiviral drugs acyclovir (ACV) and valacyclovir (VCV) and their major impurity (guanine) was developed. Under the adopted conditions (BGE of 20 mM citric acid adjusted with 1 M tris solution (pH 2.75) containing 125 mM sodium dodecyl sulphate), and analytes were all separated in about 4 min.

A CZE method for the simultaneous separation of the enantiomers of both ofloxacin and ornidazole using sulfated-β-cyclodextrin (S-β-CD) as chiral selector is also described. Good analysis time (less than 16 min) with resolution of 5.45 and 6.28 for ofloxacin and ornidazole enantiomers, respectively, were achieved using a BGE of 50 mM H_3PO_4 adjusted with 1 M tris solution; pH 1.85; containing 30 mg mL^{-1} S-β-CD. Recoveries between 97.1 – 104.0 % were obtained. The computational calculations for the enantiomeric inclusion complexes are also described.

A simple CZE assay stability-indicating method for the determination of modafinil in pharmaceutical formulations has been developed. The method showed not only good precision and accuracy but also good robustness. The LOD and LOQ were 1.2 and 3.5 μg mL^{-1}, respectively. Excipients present in the tablets and degraded products from the different stress conditions did not interfere in the assay.

A rapid CZE method was also developed and validated for the determination of the enantiomers of modafinil in less than 5 min with good resolution (Rs = 2.51) using a BGE of 25 mM H_3PO_4 adjusted with 1 M tris solution; pH 8.0; containing 30 mg mL^{-1} of S-β-CD. Computational calculations, binding constant measurements (double reciprocal, *X*-reciprocal and *Y*-reciprocal plots) as well as thermodynamic parameters were also conducted. All the above developed methods were validated, and were successfully applied to the assay of the analyte in pharmaceutical formulations.

A three-phase hollow fiber liquid-phase microextraction (HF-LPME) followed by CZE separation was successfully developed and validated for the determination of trace levels of the anti-diabetic drug, rosiglitazone (ROSI) in biological fluids. Under the optimized conditions (extraction solvent, dihexyl ether; donor phase pH, 9.5; acceptor phase, 0.1M HCl; stirring speed, 600 rpm; extraction time, 30 min; without addition of salt), enrichment factor of 280 was obtained. Good linearity and correlation coefficients of the analyte was obtained over the concentration range of 5.0 - 500 ng mL^{-1} (r^2 = 0.9967). The method is simple, sensitive and is suitable for the determination of trace amounts of ROSI in biological fluids.

CHAPTER ONE

1.1 Capillary Electrophoresis

Capillary electrophoresis (CE) is a separation technique that is carried out in capillaries under the influence of an external electric field. The separation is based on the differences in the electrophoretic mobilities of the charged species due to their charge, size, shape, nature of the background electrolyte (BGE), etc. BGE may contain additives, which can interact with the analytes and alter their electrophoretic mobilities. The separation is highly dependent on the pH of the BGE which controls the dissociation of the acidic groups on the analyte or the protonation of basic functions on the analyte (Figure 1.1) (Riekkola *et al.*, 2004).

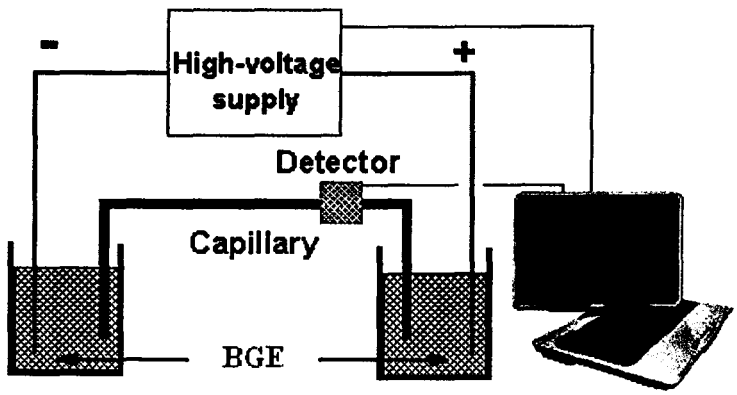

Figure 1.1 Schematic diagram of a CE instrumental set-up.

The International Union of Pure and Applied Chemistry (IUPAC) does not encourage the term "capillary electrophoresis" as an umbrella for all capillary electromigration techniques because these techniques may involve other separation mechanisms that are different from electrophoresis. CE encompasses other electromigration techniques including capillary gel electrophoresis, affinity capillary

electrophoresis, capillary isotachophoresis, capillary isoelectric focusing, micellar electrokinetic chromatography (MEKC), microemulsion electrokinetic chromatography and capillary electrochromatography (CEC) (Kašička, 2001; Riekkola *et al.*, 2004).

CEC combines the separation efficiency of CE with sample capacity and selectivity of liquid chromatography (LC). This hybrid technique was originally proposed by Pretorius *et al.*, in 1974. CEC did not attract much attention until it was demonstrated by Jorgenson and Lukacs using packed capillary in 1981 and later when Knox and Grant developed the theory in the late 1980s and the beginning of 1990s. The transportation of mobile phase through the chromatographic stationary phase in CEC is electro-driven instead of pressure-driven and therefore it offers a number of advantages such as increased efficiency and improved resolution (Liu, 2001).

CE has also been successfully coupled with many kinds of detectors such as laser induced fluorescence (LIF), (Goldsmith *et al.*, 2007); mass spectrometry (MS), (Gennaro *et al.*, 2006); chemiluminescence, (Zhao *et al.*, 2008), and more recently with capacitively coupled contacless conductivity detection (C^4D) (Nussbaumer *et al.*, 2009). The importance of coupling these detectors to CE is mainly to enhance the sensitivity of the conventional ultraviolet (UV) detector due to the short sample path length.

1.2 Theory of Electrophoretic Separation

The velocity (v) of the charged analyte in CE depends mainly on the electrophoretic mobility (μ) and the applied electric field E.

$$v = \mu E \quad \ldots\ldots\ldots\ldots\ldots\ldots \quad (1.1)$$

The velocity is controlled by two competing forces, namely, the applied electric field and the frictional force from the medium. Thus, for spherical solutes, these forces are equal but opposite once they reach the steady state. The electrophoretic mobility, (μ) can be written as follows:

$$\mu = \frac{q}{6\pi\eta r} \quad \ldots\ldots\ldots\ldots\ldots\ldots \quad (1.2)$$

where q is the charge of the molecule, η is the viscosity of the BGE and r is the analyte radius (Subramanian, 2007).

The electroosmotic flow (EOF), which contributes significantly to solute migration, is a product of mobility, (μ_{EOF}) and E:

$$v_{EOF} = \mu_{EOF} E \quad \ldots\ldots\ldots\ldots\ldots\ldots \quad (1.3)$$

where the mobility depends on the dielectric constant (ε) of the BGE and the zeta potential, (ζ):

$$\mu_{EOF} = \frac{\varepsilon\zeta}{4\pi\eta} \quad \ldots\ldots\ldots\ldots\ldots\ldots \quad (1.4)$$

pH of the BGE play an important role in controlling the silanol groups of fused-silica capillaries where it becomes deprotonated, resulting in a negative surface charge. Therefore, a double layer of rigidly adsorbed ions and diffuse layer develops and the potential of this diffuse layer is called the zeta potential (Figure 1.2). Cations in the diffuse layer will migrate towards the cathode when the electric voltage is applied, thus dragging the water layer which results in a flow towards the cathode. The EOF value can be modified by controlling the buffer pH, adding buffer additives or by coating the capillary surface. In order to achieve the separation, analytes must have different mobilities under the experimental conditions (Subramanian, 2007):

$$\Delta\mu = \mu_1 - \mu_2 \quad \ldots\ldots\ldots\ldots\ldots\ldots \quad (1.5)$$

It is well known that CE has higher efficiency than high performance liquid chromatography (HPLC) and this is mainly attributed to two main factors. First, there is no stationary phase and thus, the mass transfer resistances between the stationary and mobile phases and the other dispersion mechanisms (e.g., eddy diffusion) have been avoided. Secondly, when dealing with pressure-driven flow systems such as HPLC, a laminar flow resulted due to the frictional forces at the liquid-solid boundaries and thus, a radial velocity gradient through the tube can be found. The fluid flow velocity is highest in the middle of the tube and almost zero near the tube wall. Therefore, the peak will be broad. In electrically driven systems such as in CE, the EOF is produced homogenously along the capillary, and thus there is no gradient. The flow rate will approach zero only near the capillary wall region

(double layer region). Therefore, the peak shape obtained will much better than the hydrodynamic driven flow systems of the HPLC (Heiger, 1992).

Since a significant amount of work in this thesis deals with the separation of chiral drugs, a discussion on this topic is next presented.

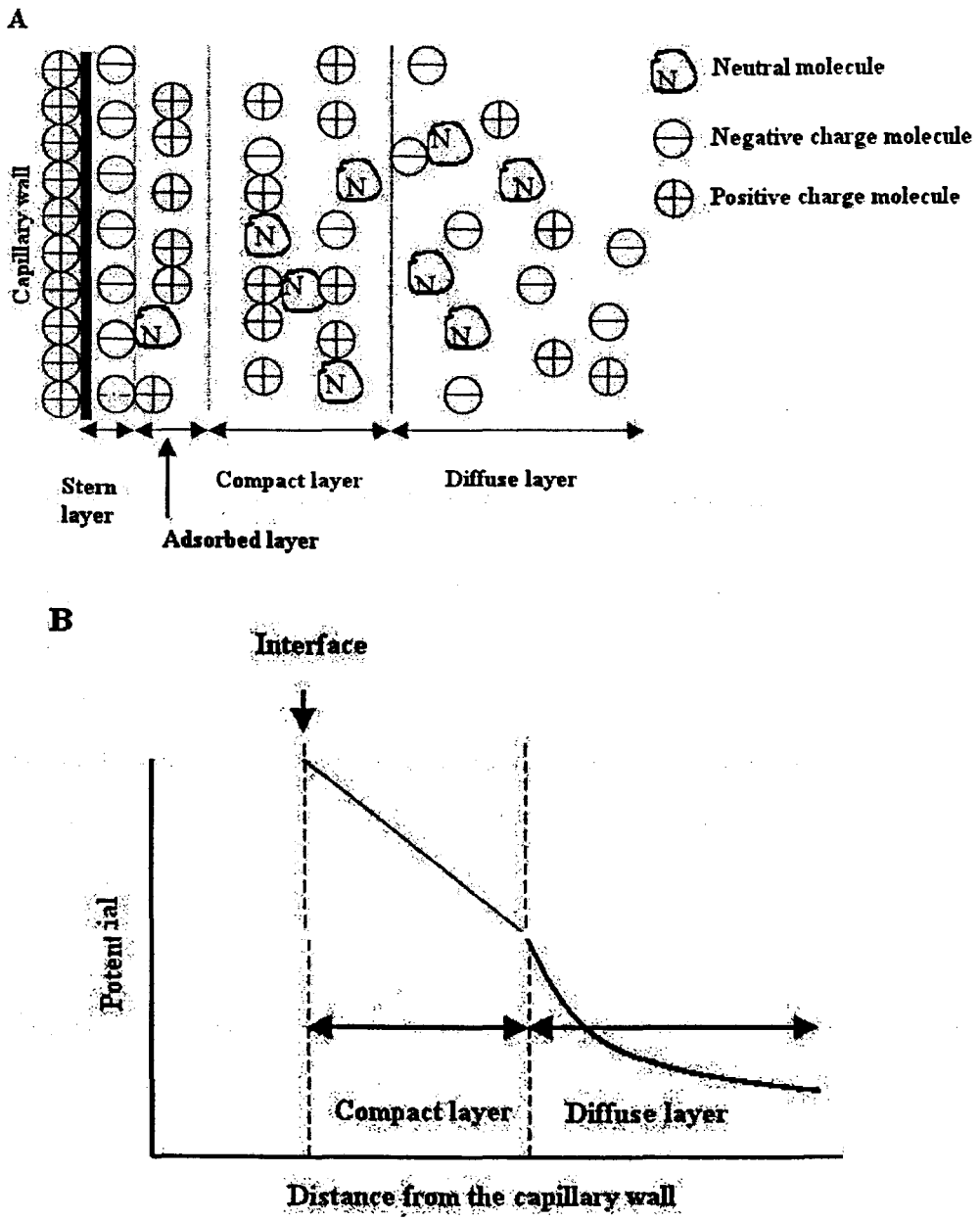

Figure 1.2 A model of a double electric layer on the interface of a silica capillary with aqueous buffer (A) and zeta potential (ζ) of the system as a function of the distance away from the wall (B) (Salomon *et al.*, 1991).

1.3 Chirality

The existence of optical isomers has been known since its discovery in 1815 by the French chemist Jean-Baptste Biot (Challener, 2001). In the early twentieth century, Cushny highlighted the importance of chirality to the pharmaceutical industry by stressing that one of the enantiomers of hyoscyamine (anticholinergic/antispasmodic) has a much higher pharmacological activity than the other (Challener, 2001; Jenkins and Hedgepeth, 2005).

"Chirality" (from the Greek word "*cheir*" for hand) means handedness which reflects the left and right-handedness of molecules (Tucker, 2000). Chiral molecules are molecules where their mirror images are not superimposable on one another, whereas, achiral compounds have superimposable mirror images. Enantiomers are two stereoisomers that have the same chemical composition and can be drawn in the same way in two dimensions. However, in chiral environments such as receptors and enzymes in the body, they act differently (McConathy and Owens, 2003). Figure 1.3 shows two forms of limonene where the (*R*)- form smells of oranges while the (*S*)-form smells of lemons (Ahlberg, 2001). Usually, the chiral center is a carbon atom where it is attached to four different groups, but there can be other sources of chirality as well (McConathy and Owens, 2003).

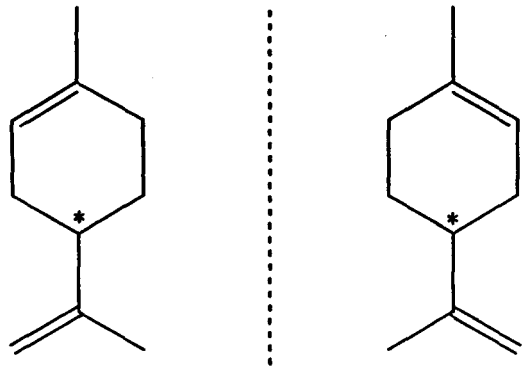

(*R*)-limonene mirror plane (*S*)-limonene

Figure 1.3 Chemical structure of the chiral limonene, (*R*)-Limonene smells of oranges and (*S*)-limonene smells of lemons (Ahlberg, 2001).

Chirality is becoming an increasingly important issue not only for pharmaceuticals but also in food, agrochemicals and the biomedical industry. Many regulatory agencies all over the world emphasize on safety and efficacy of stereoisomers in drug research and development. New guidelines from regulatory agencies also focused on single enantiomer (Challener, 2001). Sometimes during synthesis, enantiomers are produced in the same quantities, resulting in a racemate (equimolar mixture of the two enantiomers). Enantiomeric discrimination is often difficult and costly. In the past, such drugs have been marketed as racemates, despite the fact that use of single enantiomer may have numerous advantages.The other enantiomer might be inactive or without toxicological significance (Baker *et al.*, 2002, Tao and Zeng, 2002).

The development of methods for enantiomeric discrimination and for pharmacodynamic studies is attracting increasing attention. The terms "eutomer" for the more active enantiomer and "distomer" for the less active one have been suggested (Baker *et al.*, 2002).

Some examples of pharmaceuticals where one enantiomer has the desired effect while the other has adverse properties are ibuprofen (Johannsen, 2001), where the *S*-enantiomer shows pharmacological activity but the *R*-enantiomer causes unwanted side effects; ofloxacin (Awadallah *et al.*, 2003), where the antibacterial activity of *S*-enantiomer is 8 - 128 times higher than that of the *R*-enantiomer; and carvedilol (Behn *et al.*, 2001), the β-receptor blocking activity of the *S*-enantiomer is about 200-fold higher than that of *R*-carvedilol, whereas both enantiomers are equipotent α-blockers (Figure 1.4).

The current tendency of pharmaceutical industry is to switch from racemates to pure enantiomer ("chiral switching"). The advantages of taking only one form of the enantiomer are summarized below (Davies *et al.*, 2003):

(i) expose the patient to less load, thus reducing hepatic/metabolic/renal drug load,

(ii) ease of assessment of the physiology, diseases, and the administration effects,

(iii) decrease drug interactions,

(iv) avoid bioinversion, and,

(v) the ease of efficacy and toxicity assessment of the stereochemically pure active enantiomer through pharmacodynamic /pharmacokinetic monitoring studies.

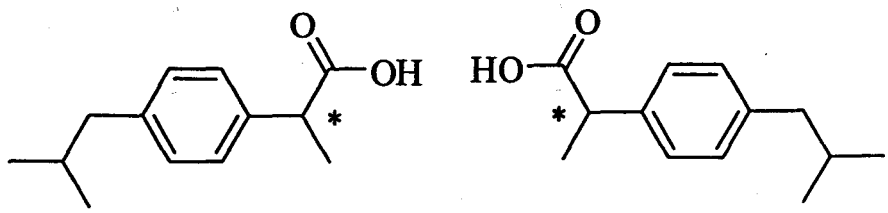

(*S*)-ibuprofen (*R*)-ibuprofen

Ibuprofen

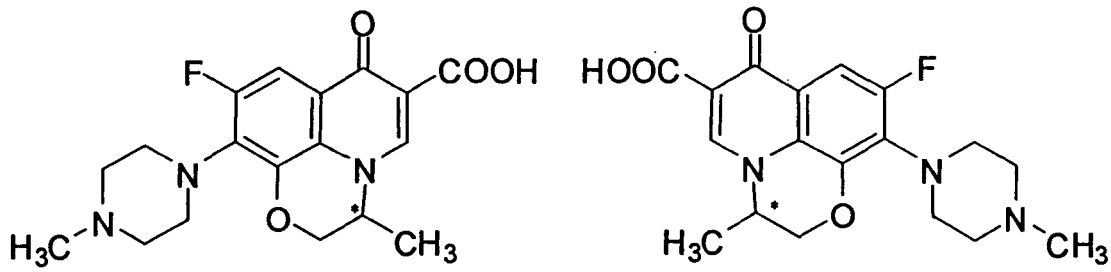

(*S*)-ofloxacin (*R*)-ofloxacin

Ofloxacin

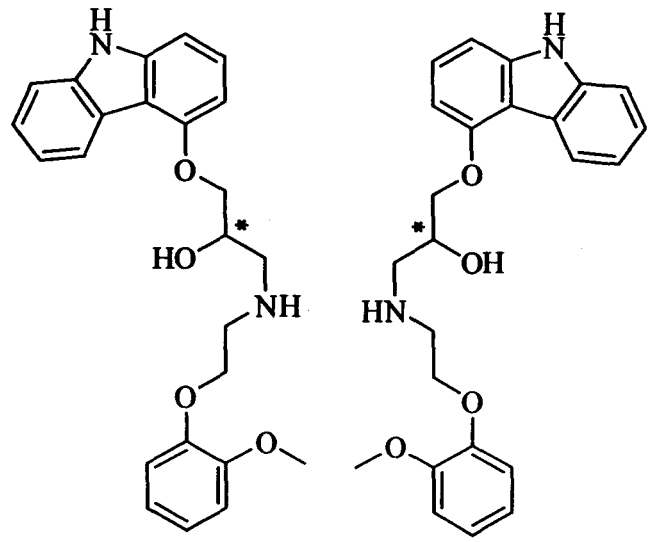

(*S*)-carvedilol (*R*)-carvedilol

Carvedilol

Figure 1.4 Chemical structures of a few chiral drugs having different effects (Johannsen, 2001; Awadallah *et al.*, 2003; Behn *et al.*, 2001).

Examples of some drugs that are produced as pure single enantiomer are shown in Figure 1.5. However, pure active enantiomer may reveal some pharmaceutical issues such as different solubility and dissolution from the analogous racemates; the possibile interaction of one enantiomer with the inert chiral excipents (e.g. cellulose derivatives) which may pose different physicochemical properties (Davies *et al.*, 2003).

1.4 Analytical Methods for the Analysis of Chiral Compounds

The Food and Drug Administration (FDA) published a guideline policy in 1992, strongly recommending companies to assess racemates and its enantiomers for newly developed drugs before being brought to the market. Therefore, developing suitable analytical methods for the resolution and determination of therapeutically active drug form is greatly needed.

Several methods for the analysis of chiral compounds are available. This include enzymatic (Baker *et al.*, 1995), thin layer chromatography (Huynh and Leipzig-Pagani, 1996; Bhushan *et al.*, 2000), nuclear magnetic resonance (Hanna and Evans, 2000; Klika *et al.*, 2010), HPLC (Akapo *et al.*, 2009), gas chromatography (Bordajandi *et al.*, 2005; Cooper *et al.*, 2009), supercritical fluid chromatography (Salvador *et al.*, 2001) and CE (Wei *et al.*, 2005; Zhao *et al.*, 2006). The earlier method has been predominantly gas chromatography (GC), but HPLC methods are being widely used now. The disadvantages of the HPLC methods will be discussed in the coming chapters (Chapters Four and Five).

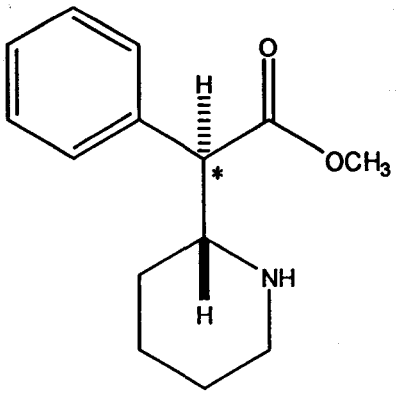

d-Threo-methylphenidate
(Central nervous system (CNS) stimulant)

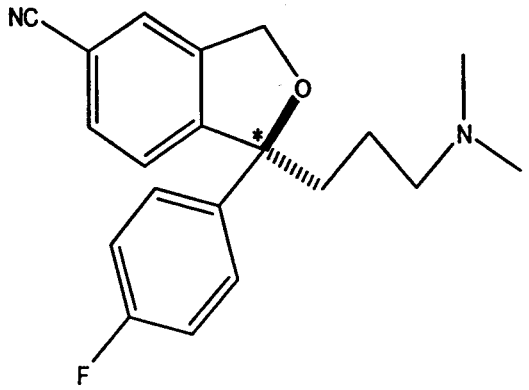

(*S*)-Citalopram
(antidepressant)

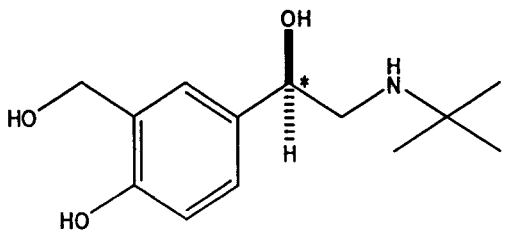

Levalbuterol
(bronchodilator)

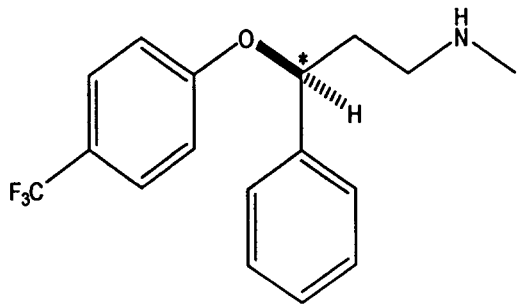

(*S*)-Fluoxetine
(antidepressant)

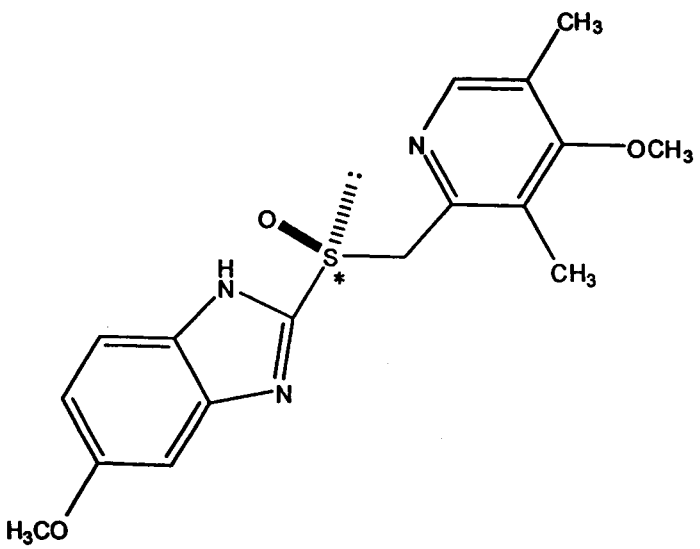

Perprazole
(antiulcerative)

Figure 1.5 Chemical structures of several stereochemically pure drugs as single enantiomers patented in the last few years (Maier *et al.*, 2001).

CE, the "youngest" separation technique for enantioseparation is simply achieved by adding the appropriate chiral selector (e.g. cyclodextrins (CDs) and their derivatives, macrocyclic antibiotics, chiral crown ethers, chiral ligand exchange, chiral ion pair reagents, chiral surfactants and miscellaneous chiral selectors) to the BGE (Fanali, 1996). The first paper on chiral CE was published by Gassman *et al.*, in 1985. A search using Scopus database search engine over the years 1985 - 2009 revealed the dramatic growth of the papers published on CE from 1996 onwards (Figure 1.6). From 1998 onwards, almost 20 % of all publications in CE deal with chiral separation.

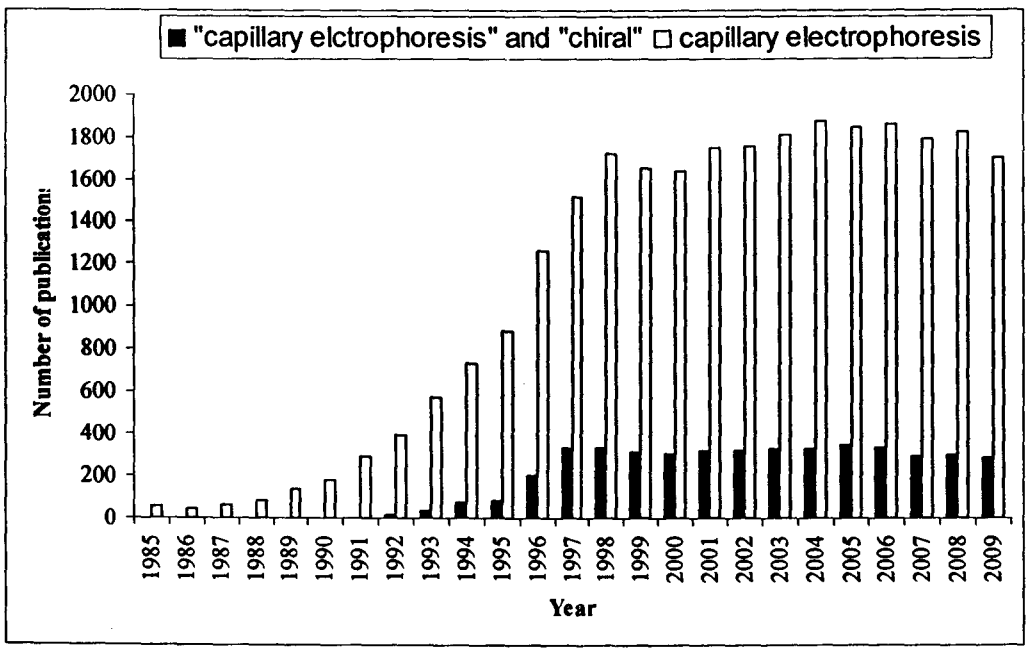

Figure 1.6 Number of CE publications since 1985. Search engine, Scopus, search keywords, "capillary electrophoresis and chiral" and "capillary electrophoresis".

The widespread acceptance of CE, is mainly due to its "green" features such as high separation efficiency, low consumption of sample and reagents (e.g., picolitèr (pL) to nanoliter (nL), often the BGE consumed is less than 1 μL for each analysis), short

analysis time, ease of operation, and can be applied to a wide range of analytes (Fanali 1996; Varenne and Descroix, 2008; Ha *et al.*, 2006; Gübitz and Schmid, 1997). One of the greatest advantages of CE compared with other analytical techniques such as HPLC is its high efficiency (theoretical plates of hundreds of thousands).

The fact that thousands of CE instruments have been installed in laboratories worldwide is clear indicators of the acceptance of the technique. It has also been implemented as an analytical technique in the United States Pharmacopeia (USP), and European Pharmacopeia (EP) (Subramanian, 2007). Regulatory authorities such as the FDA and the European Agency have accepted CE methods for the Evaluation of Medicinal Products (Subramanian, 2007).

1.5 Chiral Separation Modes

Chiral separations require the presence of a chiral selector to form transient diastereomeric complexes with the analyte. One of the inherent advantages of CE over chromatographic techniques is the fact that the chiral selector can possess an electrophoretic mobility (not possible in chromatography) and thus different schemes of migration can be applied.

In the case of neutral chiral selector, only charged analytes can be separated unless a different migration mode such as micellar electrokinetic chromatography (MEKC) is used. When separating basic analytes, an acidic (low pH) BGE is used (Figure 1.7 (A)). The basic analytes will be protonated and migrate to the detector at the

cathodic side of the capillary whereas the chiral selector does not possess any electrophoretic mobility but it is transported by the largely suppressed EOF. Therefore, the enantiomer which is complexed more strongly by the chiral selector migrates slower as it is complexed for a longer time than the more weakly bound enantiomer. Since the hydrodynamic radius of the enantiomer-CD complex is larger than the radius of the free analyte, the complex migrates slower.

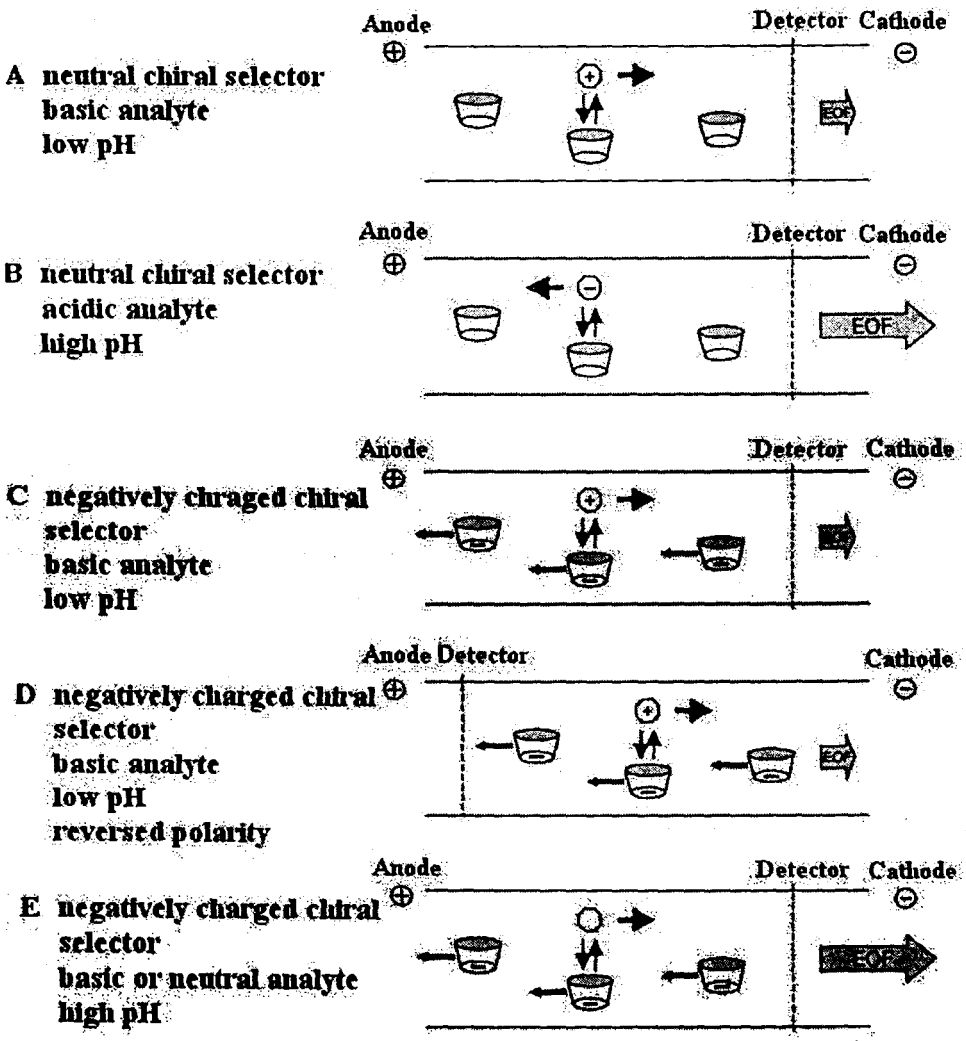

Figure 1.7 Scheme of migration modes in CE for chiral molecules (Subramaian, 2007).

In the case of separating acidic analytes and using neutral chiral selector, basic medium (high pH) is needed. The negatively charged analytes migrate to the anode but are transported to the cathodic side by the strong EOF of the basic medium. Therefore, the strongly complexed enantiomer migrates first as its mobility in the opposite direction to the detector is slowed (Figure 1.7 (B)).

Using charged chiral selectors offer additional advantages as they possess electrophoretic mobility, and thus neutral compounds can be separated. Analyzing the basic analytes using negatively charged selectors can be achieved using acidic BGE where the negatively charged chiral selector migrates to the anodic side while the positively charged basic analytes migrates towards the cathodic side (Figure 1.7 (C)).

A major advantage of using chiral selectors with opposite charge to the analytes is their counter mobility which allows the use of low concentrations of the respective chiral selector. When the chiral selector concentrations are high or the binding of the analyte enantiomers to the selector is strong, the complex may not reach the detector at the cathodic side due to the fact that the solute is transported by the negatively charged chiral selector to the anode. Therefore, voltage polarity is reversed and the detection can take place at the anodic end of the capillary (Figure 1.7 (D)) (a feature used in Chapter Four). The stronger complex that forms between the enantiomer and the chiral selector is thus detected first as it is accelerated towards the anodic side by the negatively charged selector. Compared with the situation described in (Figure 1.7 (C)), a reversal of the enantiomer migration order is observed. This situation can also be applied for the enantioseparation of neutral analytes, where the enantiomers are

transported towards the detector at the anodic side by the effect of the charged selector, with the more strongly complexed enantiomer migrating first.

Under basic conditions, charged chiral selectors may also be applied to the enantioseparation of basic and neutral analytes using the normal polarity mode (Figure 1.7 (E)) (a feature used in Chapter Five). Under basic conditions, the basic analytes are uncharged and thus transported to the detector at the cathodic side as neutral analytes. The anionic selector migrating towards the anodic side decelerates the more strongly complexed enantiomer compared with the weakly complexed enantiomer. Therefore, the weakly bound enantiomer is detected first. Anionic analytes usually exhibit only weak interactions with the negatively charged selectors due to electric repulsion and therefore are not included in the above mentioned consideration, whereas positively charged chiral selectors are useful for the enantioseparation of acidic and neutral analytes (Subramanian, 2007).

Under the normal set-up, both the capillary and the buffer reservoirs are filled with the BGE containing the chiral selector. When the chiral selector used has high UV absorbance, it will interfere with the UV detection and consequently other conditions need to be considered. The same situation is applied when the CE is coupled to a mass spectrometer where the selector entering the ion source and will accumulate inside and reduce the ionization efficiency. In view of these obstacles, the partial filling technique can be applied (Subramanian, 2007). In this technique, only part of the capillary (shorter than the effective length) is filled with the BGE containing the chiral selector, the reminder of the capillary containing chiral selector free BGE. After the injection of analyte takes place, the ends of the capillary are immersed in

selector-free BGE and the voltage is applied which results in the migration of the charged analytes through the selector-containing BGE zone where they are separated. At the end, the enantiomers enter the selector-free BGE zone and migrate to the detector (Amini *et al.*, 1999). The conditions need to be adjusted to assure that the selector zone does not migrate towards the detector to a significant extent due to the high EOF. Generally, the selector zone is immobile but in any case the analyte must migrate faster than the selector zone in order to reach detector before the selector zone (Subramanian, 2007).

The counter current technique is appropriate when using chiral selectors with opposite charge to the analytes for cationic analytes and negatively charged chiral selectors. In this technique, the whole capillary may be filled with the chiral selector-containing BGE. Once the analyte is injected, the separation is achieved using selector-free BGE in the cathodic BGE reservoir and whether the selector-free or selector-containing BGE in the anodic reservoir. Due to its negative charge, the chiral selector migrates to the anodic side clearing the detection zone and thus the analytes which are separated while migrating through the selector zone to the cathodic side are detected in the absence of the chiral selector. Interestingly, the combination of the two techniques is possible, where partial filling of the capillary with a selector migrating in the opposite direction of the analytes (Subramaian, 2007).

1.6 Chiral Selectors

A large number of chiral selectors are currently available, and continue to increase. Therefore, choosing the best chiral selector for a specific purpose can be a difficult

issue. Usually, the suitable chiral selector is selected by trial and error and this can be expensive and time consuming. Some of the common chiral selectors are next discussed.

1.6.1 Proteins

The rational of using proteins as chiral selectors came from the fact that drugs binds stereoselectively to proteins and therefore led to investigations of using these proteins as chiral selectors (Gübitz and Schmid, 2000). The simplest way of using proteins as chiral selectors is to dissolve it in the BGE. Examples of these proteins are human and porcine serum albumin, bovine serum albumin (BSA) which is added to the BGE using the partial-filling technique. Proteins can also be covalently bounded to silica materials in CE, or to the inner surface of the coated capillary. Alternatively, the simple dynamic coating approach of the capillary wall can also be used (Ha *et al.*, 2006).

Problems associated with the use of proteins as chiral selectors are the adsorption of the chiral selector to the capillary wall and the UV absorption interferences. These two problems can limit the use of these proteins as chiral selectors. A few approaches can be used to overcome these problems. For instance, to eliminate the adsorption to the capillary wall, the capillary can be modified and this can be achieved either by dynamic modification, adsorption of polymers to the capillary wall or covalent bonding of functional group to silanol sites (Amini, 2001). For UV absorption problem, the partial-filling technique can be used (Gübitz and Schmid, 2000). In order to protect the natural conformations of proteins for the purpose of chiral separation, mild methods for immobilization onto matrices are needed (e.g.,

sol-gel encapsulation, physical adsorption and covalently binding) (Zhang *et al.*, 2010).

1.6.2 Polysaccharides

Linear, neutral and charged polysaccharides, e.g., chondroitin sulfates, dextrans, dextrins, aminoglycosides and heparin (Figure 1.8) have also been used as chiral selectors in HPLC and CE (Blanco and Valverde, 2003; Amini, 2001). It has been reported that the complexation between the analyte and polysaccharides is weaker than in CDs, and this may be attributed to the weaker hydrophobic interactions (Amini, 2001). The mechanism of enantioseparations is based on the conformation changes from a flexible coil to a helix in the presence of an analyte and buffer salts. The helical structure forms a hydrophobic cavity, mimicking a CD cavity, in which the analyte can be included; the formed cavity is more flexible than that of CDs (Amini, 2001). Two different groups of carbohydrates can be distinguished: neutral and charged oligo-and polysaccharides. Neutral carbohydrates such as dextrins (Soini *et al.*, 1994; Nishi and Kuwahara, 2001) and dextrans (Nishi and Kuwahara, 2001) whereas negatively charged polysaccharides such as heparin, dextran sulphate, chondroitin sulphate C and A have been shown to be suitable as chiral selectors for basic drugs (Nishi, 1997; Nishi and Kuwahara, 2001).

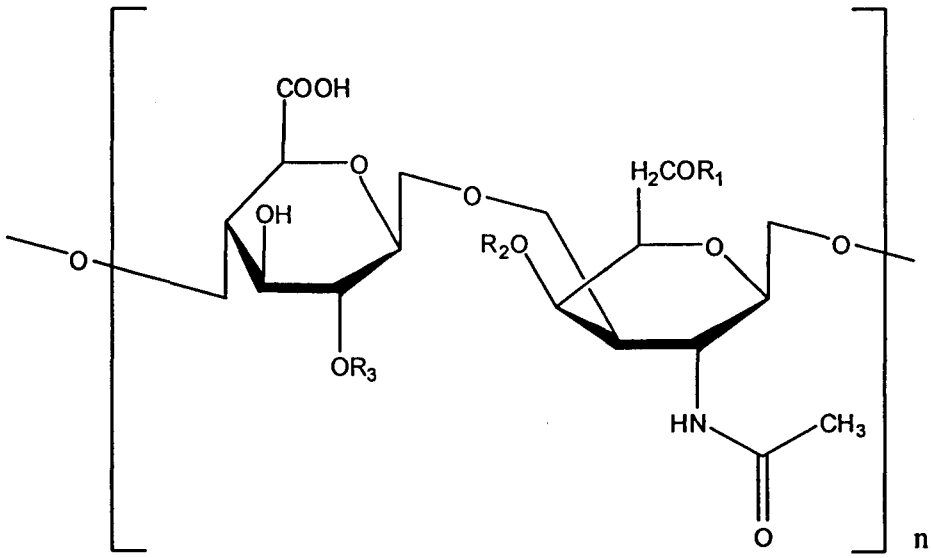

Chondroitin sulfate

Chondroitin-4-sulfate (Chondroitin sulfate A): R_1 = H; R_2 = SO_3H; R_3 = H.
Chondroitin-6-sulfate (Chondroitin sulfate C): R_1 = SO_3H; R_2, R_3 = H.

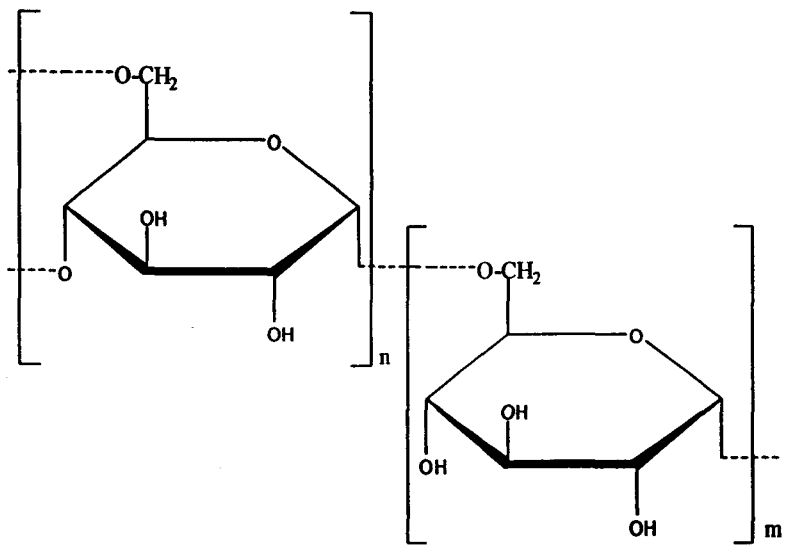

Dextran

Figure 1.8 Chemical structures of some polysaccharides used as chiral selectors

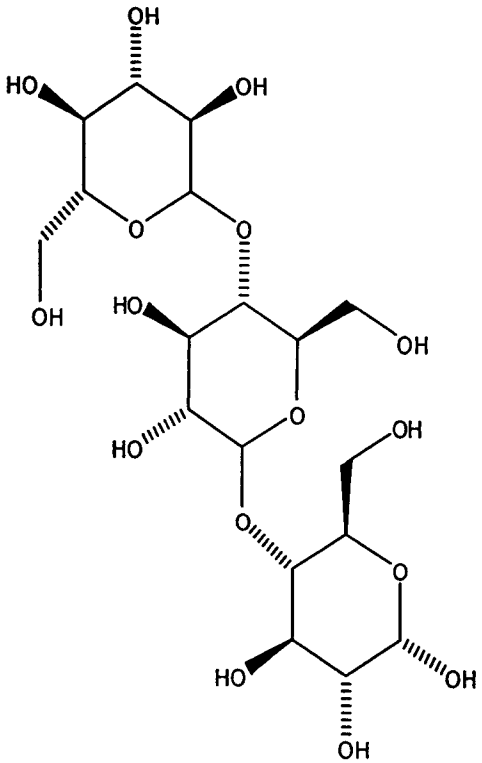

Dextrin

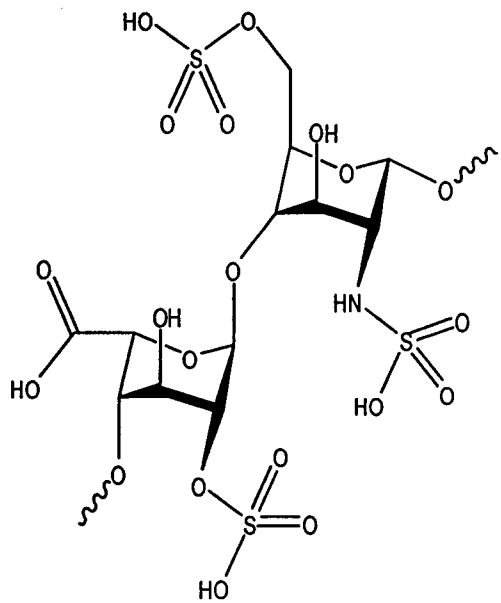

Heparin

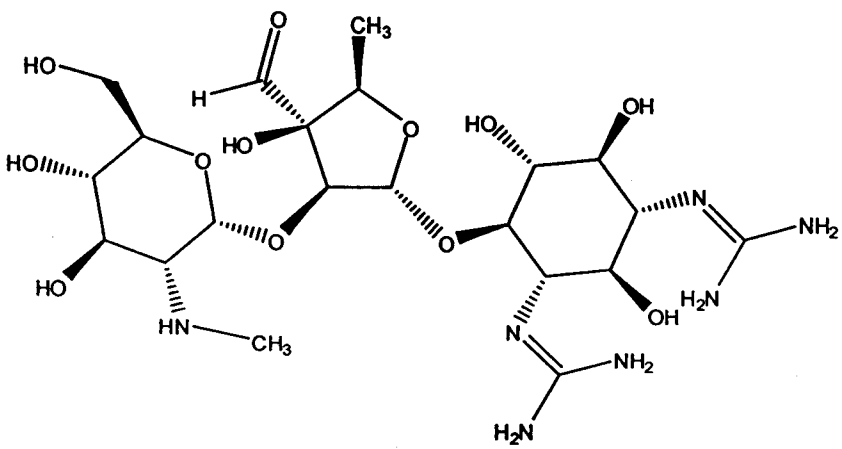

Aminoglycosides

Figure 1.8. Continued

1.6.3 Macrocyclic Antibiotics

Several macrocyclic antibiotics e.g., ansa compounds (ansamycins) and glycopeptides antibiotics (e.g., vancomycin, teicoplanin, ristocetin A, avoparcin and balhimycin) have been used as chiral selectors in CE. (Desiderio and Fanali, 1998; Blanco and Valverde, 2003). Ansa compounds consisting of a chromophore bonded to a hydrocarbon chain bearing different substituents. While glycopeptides consist of three or four fused macrocyclic rings composed of linked amino acids and substituted phenols. Some fused rings bear various sugar or saccharide moieties. Both the ansa and glycopeptides share similar structural features such as the presence of several stereogenic centers and many functional groups, permitting multiple interactions with the analytes. Other interactions such as ionic, hydrogen bonding, dipole-dipole, π-π, hydrophobic and steric repulsion are assumed to take place to enantioresolve analytes with widely different structures (Blanco and Valverde, 2003; Gübitz and Schmid, 2000; Zhang *et al.*, 2010).

As these macrocyclic antibiotics have aromatic moieties, thus they have strong UV absorption up to 250 nm, so partial filling or counter current techniques is deemed necessary for obtaining sensitive assays (Gübitz and Schmid, 2000). Other limitations for these compounds are their lack of stability in aqueous solutions compared to anhydrous form (e.g., the aqueous solution of vancomycin at pH 5 - 7 deteriorates within 2 - 4 days at room temperature and 6 - 7 days at 4 °C) (Armstrong and Nair, 1997).

1.6.4 Ligand Exchangers

Chiral ligand exchange enantioseparation is mainly attributed to the thermodynamic stability difference of the ternary metal complexes that are formed between the chiral selector and analyte. Chiral ligand exchangers are effective for the enantioseparation, especially for the amino acids with high selectivity (Zhang *et al.*, 2010). Enantioseparation using ligand-exchange complexation is based on the formation of diastereomeric transient mixed metal complexes (usually Cu (II), also Ni (II) or Zn (II)) between at least two chiral bifunctional ligands (usually L-amino acids) and the analyte enantiomers (Figure 1.9) (Blanco and Valverde, 2003).

The concentration of the metal and the ligand must be suitable, i.e., the concentration of the ligand is twice that of the metal ion. Enantioseparation is based on the different stability constants of the diastereomeric complexes. The analyte and ligand form a ternary complex as follows (Amini, 2001):

$$[L]_n\text{-}[M] + [E] \leftrightarrow [L]_{n-1}\text{-}[M] - [E] + [L] \quad . \; . \; . \quad (1.6)$$

where L is the chiral ligand, M is the metal ion and E is the enantiomer.

Chiral ligand exchange has been successfully applied for the enantioseparation of the free and *N*-derivatized amino acids, dipeptides, α-hydroxy acids and amino alcohols such as sympathomimetics and β-blockers (Subramanian, 2007). Mizrahi *et al.*, (2008), reported the enantioseparation of five pairs of dansylated amino acids in a *trans*-(1S,2S)-1,2-bis-(dodecylamido) cyclohexane organogel using a complex of D-valine and copper as the selector by the ligand exchange CEC (Zhang *et al.*, 2010).

Disadvantages of the ligand-exchange as chiral selectors are mainly due to their limited stability and the detection difficulties resulting from their UV absorption (Vespalec and Boček, 2000).

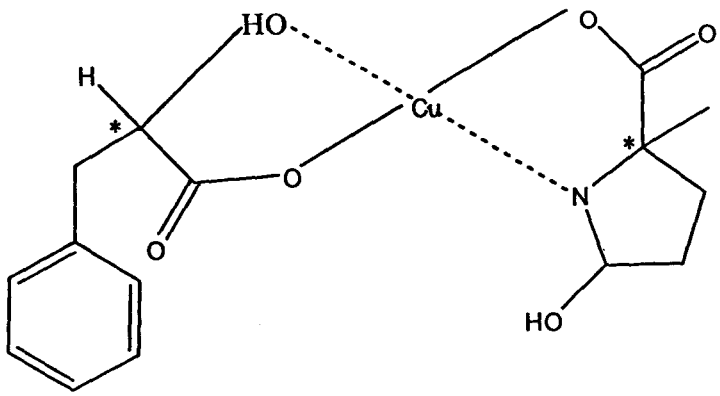

L-3-phenyl-lactic acid L-hydroxyproline

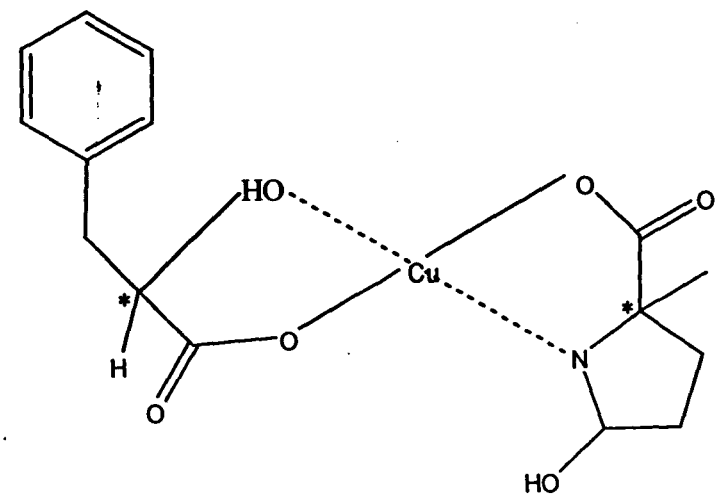

D-3-phenyl-lactic acid L-hydroxyproline

Figure 1.9 Possible structures for the ternary complexes formed between the enantiomers of 3-phenyl-lactic acid and L-hydroxyproline (Blanco and Valverde, 2003).